MIXED CONVECTION FLOW AT THE LOWER STAGNATION POINT OF A CIRCULAR CYLINDER EMBEDDED IN A POROUS MEDIUM FILLED BY A NANOFLUID CONTAINING GYROTACTIC MICROORGANISMS

(Aliran Olakan Campuran pada Titik Genangan Bawah Silinder Bulat yang Dibenam dalam Medium Berliang dengan Nanobendalir yang Mengandungi Mikroorganisma Gyrotactic)

LEONY THAM YEW SENG, ROSLINDA NAZAR & IOAN POP

ABSTRACT

In this paper, the steady mixed convection boundary layer flow near the lower stagnation point of a horizontal circular cylinder with a constant surface temperature embedded in a porous medium saturated by a nanofluid containing gyrotactic microorganisms in a stream flowing vertically upwards for both cases of a heated and cooled cylinder, is studied numerically. The resulting system of nonlinear ordinary differential equations is solved numerically using an implicit finite-difference scheme known as the Keller box method. By considering the governing parameters, namely the mixed convection parameter λ, the bioconvection Lewis number *Lb*, the traditional Lewis number *Le*, the bioconvection Péclet number *Pb*, the buoyancy ratio *Nr*, the bioconvection Rayleigh number *Rb*, the Brownian motion *Nb* and the thermophoresis *Nt*, the numerical results are obtained and discussed for the skin friction coefficient, the local Nusselt number, the local Sherwood number, the local density number of the motile microorganisms as well as the velocity, temperature, nanoparticles volume fraction and motile microorganisms density profiles.

Keywords: bioconvection; horizontal circular cylinder; lower stagnation point; mixed convection; nanofluid; porous medium

ABSTRAK

Dalam makalah ini, aliran lapisan sempadan olakan campuran mantap pada titik genangan bawah silinder bulat mengufuk dengan suhu permukaan malar yang dibenam dalam medium berliang yang dipenuhi nanobendalir dan mengandungi mikroorganisma gyrotactic, dalam aliran yang mengalir menegak ke atas bagi kedua-dua kes silinder yang dipanaskan dan disejukkan, telah dikaji secara berangka. Sistem persamaan pembezaan biasa tak linear yang terhasil diselesaikan secara berangka menggunakan skema beza terhingga tersirat yang dikenali sebagai kaedah kotak Keller. Dengan mempertimbangkan beberapa parameter menakluk, iaitu parameter olakan campuran λ, nombor Lewis bio-olakan *Lb*, nombor Lewis tradisional *Le*, nombor Péclet bio-olakan *Pb*, nisbah keapungan *Nr*, nombor Rayleigh bio-olakan *Rb*, gerakan Brownan *Nb* dan termoforesis *Nt*, keputusan berangka diperoleh dan dibincangkan bagi pekali geseran kulit, nombor Nusselt setempat, nombor Sherwood setempat, nombor ketumpatan setempat bagi mikroorganisma motil serta profil-profil halaju, suhu, pecahan isi padu nanozarah dan ketumpatan mikroorganisma motil.

Kata kunci: bio-olakan; silinder bulat mengufuk; titik genangan bawah; olakan campuran; nanobendalir; medium berliang

1. Introduction

The combined convective heat transfer in fluid saturated porous media is important in the area related to fibrous insulation, food processing and storage, thermal insulation of buildings, geophysical systems, electro chemistry and nuclear reactors. A comprehensive concepts and

applications of porous media are well documented in the books by Nield and Bejan (2006), Ingham and Pop (2005) and Vafai (2005). Merkin (1977) and Cheng (1982) are the pioneers in the study related to porous media problems. The studies were followed by a series of investigations by Badr and Pop (1988, 1992), Bradean *et al.* (1998) and Kumari and Pop (2009).

The term nanofluid has been introduced by Choi (1995), to define the dilution of nanometer-sized particles, which is smaller than 100nm, in a base fluid (Das *et al.* 2007), such as water, ethylene glycol and oil. These nanometer-sized particles allow the nanoparticles to flow easily through the microchannels (Khanafer *et al.* 2003), and they possess a higher thermal conductivity property, making the nanofluid to be an impressive enhancement of thermal conductivity and heat transfer compared to the base fluid only (Sadik and Pramuanjaroenkij 2009). As such, the nanofluids are potentially contributing in microfluidic devices (Kuznetsov 2010). Many solid and comprehensive references on nanofluids are available, such as the book by Das *et al.* (2007), review papers by Buongiorno (2006), Duangthongsuk and Wongwises (2007), Wang and Mujumdar (2008), Kakaç and Pramuanjaroenkij (2009), and Nazar *et al.* (2011). On the other hand, Tsai *et al.* (2009) found that mixing nanoparticles in the base fluid is an issue, and that nanofluid itself, without a stabiliser, nanoparticles in nanofluid are unstable, and have the tendency to aggregate and causing the clogging of microchannels and decreasing the thermal conductivity of nanofluid. For the instability issue in nanofluid, by introducing the upswimming microorganisms that are heavier than water (base fluid), these microorganisms, such as gyrotactic microorganisms like algae, which tend to concentrate in the upper portion of the fluid layer thus causing a top-heavy density stratification that often becomes unstable (Pedley *et al.* 1988; Ghasemi & Aminossadati 2010), and causing a bioconvection to occur in this nanofluid flow, and eventually increasing the stability of nanoparticles to suspend, which could avoid nanoparticles from agglomerating and aggregating (Yu 2012).

Bioconvection is a phenomenon that occurs when convection instability is induced by upswimming microorganisms that are heavier than water. By bioconvection motion introduced in nanofluids, besides solving the instability issue and improving the suspension of nanoparticles (Kuznetsov 2011), the mixing nanoparticles issue could also be resolved, and these could enhance mass transfer in microvolumes (Sokolov *et al.* 2009; Tsai *et al.* 2009). Aziz *et al.* (2012) have numerically studied for free convection boundary layer flow past a horizontal flat plate, with nanofluid containing gyrotactic microorganisms, and found that the bioconvection parameters strongly influenced the mass, heat, and motile microorganisms transport rate.

In this paper, we combine the nanofluid equation model proposed by Buongiorno (2006) and the transformations proposed by Merkin (1977), with the present study limited to the case near the lower stagnation point of the cylinder, namely the steady laminar mixed convection boundary layer flow near the lower stagnation point of a horizontal circular cylinder embedded in a porous medium filled by a nanofluid containing gyrotactic microorganisms. The aim of this study is to understand the behaviour of nanofluid suspensions containing gyrotactic microorganisms at the fundamental level. The resulting nonlinear boundary layer equations are solved numerically using an efficient implicit finite-difference scheme, known as the Keller-box method, which is described in the book by Cebeci and Bradshaw (1984). The variations of the skin friction coefficient, local Nusselt number, local Sherwood number, local density number of the motile microorganisms as well as the velocity, temperature, nanoparticles volume fraction and density motile microorganisms profiles, for various values of the governing parameters, namely the mixed convection parameter, bioconvection Lewis number, traditional Lewis number, bioconvection Péclet number, buoyancy ratio parameter, bioconvection Rayleigh number, Brownian motion parameter and thermophoresis parameter, are investigated and illustrated through tables and figures. For comparison purposes, the present results are

compared with previously published results for the regular Newtonian fluid case (Cheng 1977; Nazar *et al.* 2003), and it is found that the comparisons show excellent agreement.

2. Basic Equations

We consider the steady mixed convection boundary layer flow past a heated or cooled horizontal circular cylinder of radius a embedded in a porous medium filled by a water-based nanofluid containing nanoparticles and gyrotactic microorganisms. The nanoparticle suspension is assumed to be stable (there is no nanoparticle agglomeration). There are experimental techniques that make it possible to prepare nanoparticle suspensions that remain stable for several weeks. The presence of nanoparticles is assumed to have no effect on the direction of microorganisms' swimming and on their swimming velocity. This is a reasonable assumption if the nanoparticle suspension is dilute (nanoparticle concentration is less than 1%). Bioconvection induced flow is expected to occur only in a dilute suspension of nanoparticles; otherwise, a large concentration of nanoparticles would result in a large suspension viscosity, which would suppress bioconvection. It is assumed that the uniform temperature, the uniform nanoparticle volume fraction and the uniform density of motile microorganisms of the surface of the cylinder are $\overline{T}_w$, $\overline{C}_w$ and $\overline{n}_n$, while the ambient values, attained as $\overline{y}$ tends to infinity are $\overline{T}_\infty$, $\overline{C}_\infty$ and $\overline{n}_\infty$, where $T_w > T_\infty$ for a heated cylinder (assisting flow) and $T_w < T_\infty$ for a cooled cylinder (opposing flow). It is also assumed that the velocity of the external flow (inviscisd flow) is $\overline{u}_e(\overline{x})$, where $\overline{x}$ is the coordinate measured along the surface of the cylinder starting from the lower stagnation point and $\overline{y}$ is the coordinate measured in the direction normal to the surface of the cylinder. Further, it is assumed that the Oberbeck-Boussinesq approximation takes place and that the nanoparticle concentration is dilute. Under these assumptions, the governing equations, based on the models proposed by Buongiorno (2006) and Kuznetsov (2010), are

Continuity equation:

$$\overline{\nabla} \cdot \overline{\mathbf{v}} = 0 \tag{1}$$

Momentum (Darcy) equation:

$$\frac{\mu}{K}\overline{\mathbf{v}} = -\overline{\nabla}\,\overline{p} + \left\{\overline{C}\,\rho_p + (1-\overline{C})\,\rho_{f\infty}\left[1-\beta(\overline{T}-\overline{T}_\infty)\right] + \overline{n}\,\gamma\Delta\rho\right\}\mathbf{g} \tag{2}$$

Thermal energy equation:

$$\overline{\mathbf{v}} \cdot \overline{\nabla}\overline{T} = \alpha_m \overline{\nabla}^2\overline{T} + \tau\left[D_B \overline{\nabla}\overline{T} \cdot \overline{\nabla}\overline{C} + (D_T / \overline{T}_\infty)\overline{\nabla}\overline{T} \cdot \overline{\nabla}\overline{T}\right] \tag{3}$$

Oxygen conservation equation:

$$\overline{\mathbf{v}} \cdot \overline{\nabla}\overline{C} = D_B \overline{\nabla}^2\overline{C} + \left(D_T / \overline{T}_\infty\right)\overline{\nabla}^2\overline{T} \tag{4}$$

Conservation equation for microorganisms:

$$\overline{\nabla} \cdot \overline{\mathbf{j}} = 0 \tag{5}$$

where $\overline{\mathbf{j}}$ is the flux of microorganisms, which is defined as

$$\overline{\mathbf{j}} = \overline{n}\,\overline{\mathbf{v}} + \overline{n}\,\tilde{\overline{\mathbf{v}}} - D_n \overline{\nabla}\,\overline{n} \tag{6}$$

In keeping with the Oberbeck-Boussinesq approximation and an assumption that the nanoparticle concentration is dilute, and with a suitable choice for the reference pressure, we can linearise the momentum equation and write Eq. (2) as

$$\frac{\mu}{K}\overline{\mathbf{v}} = -\overline{\nabla}\,\overline{p} + \left[(\rho_p - \rho_{f\infty})(C - C_\infty) - (1-\overline{C})\rho_{f\infty}\beta(\overline{T} - \overline{T}_\infty) + \overline{n}\,\gamma\,\Delta\rho\right]\mathbf{g} \tag{7}$$

Here $\overline{\mathbf{v}}$ is the fluid filtration velocity, $\tilde{\overline{\mathbf{v}}}$ is the average directional swimming velocity of a microorganism, $\overline{T}$ is the temperature, $\overline{C}$ is the oxygen concentration, $\overline{p}$ is the pressure, $\overline{n}$ is the density of motile microorganisms, $\mathbf{g}$ is the gravity vector, K is the permeability of the porous medium, α_m is the effective thermal diffusivity of the porous medium, μ and β are the viscosity and volume expansion coefficient of the fluid, ρ_p is the density of the particles, $\Delta\rho = \rho_{\mathrm{m}\infty} - \rho_{\mathrm{f}\infty}$ is the density difference between the microorganism density, $\rho_{\mathrm{m}\infty}$, and the base fluid density, $\rho_{\mathrm{f}\infty}$, γ is the average volume of a microorganism, D_B is the Brownian diffusion coefficient, D_T is the thermophoretic diffusion coefficient of the microorganisms, D_n is the diffusivity of microorganisms, $\overline{\nabla}^2$ is the Laplacian operator and $\tau = (\rho c)_p / (\rho c)_f$ with $(\rho c)_p$ being the effective heat capacity of the nanoparticle material and $(\rho c)_f$ is the heat capacity of the fluid. We notice that $\tilde{\overline{\mathbf{v}}}$ can be approximated as

$$\tilde{\overline{\mathbf{v}}}(\tilde{\overline{u}}, \tilde{\overline{v}}) = (bW_c / \Delta\overline{C})\overline{\nabla}\,\overline{C} \tag{8}$$

where $\tilde{\overline{u}} = (bW_c / \Delta\overline{C})\partial\overline{C}/\partial\overline{x}$ and $\tilde{\overline{v}} = (bW_c / \Delta\overline{C})\partial\overline{C}/\partial\overline{y}$. Further, $\Delta\overline{C} = \overline{C}_w - \overline{C}_\infty$ is the characteristic nanoparticle volume fraction, b is the chemotaxis constant [m] and W_c is the maximum cell swimming speed [m/s] (the product bW_c is assumed to be constant). The buoyancy term due to microorganisms' upswimming in the momentum (Darcy) Eqs. (2) and (7) are based on the papers by Hillesdon and Pedley (1996), Eqs. (1), (3-5) and (7) can be written in the Cartesian coordinates as

$$\frac{\partial\overline{u}}{\partial\overline{x}} + \frac{\partial\overline{v}}{\partial\overline{y}} = 0 \tag{9}$$

$$\frac{\mu}{K}\overline{u} = -\frac{\partial\overline{p}}{\partial\overline{x}} + \left[(1-\overline{C}_\infty)\rho_{f\infty}\beta(\overline{T} - \overline{T}_\infty) - (\rho_p - \rho_{f\infty})(\overline{C} - \overline{C}_\infty) - \overline{n}\,\gamma\,\Delta\rho\right]g\sin(\overline{x}/a) \tag{10}$$

$$\frac{\mu}{K}\overline{v} = -\frac{\partial\overline{p}}{\partial\overline{x}} - \left[(1-\overline{C}_\infty)\rho_{f\infty}\beta(\overline{T} - \overline{T}_\infty) - (\rho_p - \rho_{f\infty})(\overline{C} - \overline{C}_\infty) - \overline{n}\,\gamma\,\Delta\rho\right]g\cos(\overline{x}/a) \tag{11}$$

$$\overline{u}\frac{\partial \overline{T}}{\partial \overline{x}}+\overline{v}\frac{\partial \overline{T}}{\partial \overline{y}}=\alpha_m\left(\frac{\partial^2 \overline{T}}{\partial \overline{x}^2}+\frac{\partial^2 \overline{T}}{\partial \overline{y}^2}\right)+\tau\left\{D_B\left(\frac{\partial \overline{T}}{\partial \overline{x}}\frac{\partial \overline{C}}{\partial \overline{x}}+\frac{\partial \overline{T}}{\partial \overline{y}}\frac{\partial \overline{C}}{\partial \overline{y}}\right)+\left(\frac{D_T}{\overline{T}_\infty}\right)\left[\left(\frac{\partial \overline{T}}{\partial \overline{x}}\right)^2+\left(\frac{\partial \overline{T}}{\partial \overline{y}}\right)^2\right]\right\} \tag{12}$$

$$\overline{u}\frac{\partial \overline{C}}{\partial \overline{x}}+\overline{v}\frac{\partial \overline{C}}{\partial \overline{y}}=D_B\left(\frac{\partial^2 \overline{C}}{\partial \overline{x}^2}+\frac{\partial^2 \overline{C}}{\partial \overline{y}^2}\right)+\left(\frac{D_T}{\overline{T}_\infty}\right)\left(\frac{\partial^2 \overline{T}}{\partial \overline{x}^2}+\frac{\partial^2 \overline{T}}{\partial \overline{y}^2}\right) \tag{13}$$

$$\frac{\partial}{\partial \overline{x}}\left[\overline{n}\,\overline{u}+\overline{n}\,\tilde{\overline{u}}-D_n\left(\frac{\partial \overline{n}}{\partial \overline{x}}+\frac{\partial \overline{n}}{\partial \overline{y}}\right)\right]+\frac{\partial}{\partial \overline{y}}\left[\overline{n}\,\overline{v}+\overline{n}\,\tilde{\overline{v}}-D_n\left(\frac{\partial \overline{n}}{\partial \overline{x}}+\frac{\partial \overline{n}}{\partial \overline{y}}\right)\right]=0 \tag{14}$$

subject to the boundary conditions

$$\begin{aligned}&\overline{v}(\overline{x},\overline{y})=0,\quad \overline{T}(\overline{x},\overline{y})=\overline{T}_w,\quad \overline{C}(\overline{x},\overline{y})=\overline{C}_w,\quad \overline{n}(\overline{x},\overline{y})=\overline{n}_w \quad \text{at} \quad \overline{y}=0,\quad 0\le\overline{x}\le\pi\\ &\overline{u}(\overline{x},\overline{y})\to\overline{u}_e(\overline{x}),\ \overline{T}(\overline{x},\overline{y})\to\overline{T}_\infty,\ \overline{C}(\overline{x},\overline{y})\to\overline{C}_\infty,\ \overline{n}(\overline{x},\overline{y})\to\overline{n}_\infty \text{ as } \overline{y}\to\infty,\ 0\le\overline{x}\le\pi\end{aligned} \tag{15}$$

where $\overline{u}_e(\overline{x})=U_\infty \sin(\overline{x}/a)$. We introduce now the non-dimensional variables defined as

$$\begin{aligned}&x=\overline{x}/a,\quad y=Pe^{1/2}(\overline{y}/a),\quad u=\overline{u}/U_\infty,\quad v=Pe^{1/2}(\overline{v}/U_\infty)\\ &T=(\overline{T}-\overline{T}_\infty)/\Delta\overline{T},\quad C=(\overline{C}-\overline{C}_\infty)/\Delta\overline{C},\quad n=(\overline{n}-\overline{n}_\infty)/\Delta\overline{n}\end{aligned} \tag{16}$$

where $Pe=U_\infty a/\alpha_m$ is the Péclet number, α_m is the effective thermal diffusivity of the porous medium, $\Delta\overline{T}=\overline{T}_w-\overline{T}_\infty$ is the characteristic temperature, $\Delta\overline{n}=\overline{n}_w-\overline{n}_\infty$ is the characteristic of the density motile microorganisms. Eliminating $\overline{p}$ from Eqs. (10-11) by cross-differentiation, substituting (16) into the resulting equation, and considering the boundary layer approximation ($Pe\to\infty$), we obtain the following boundary layer equations for the problem under consideration:

$$\frac{\partial u}{\partial x}+\frac{\partial v}{\partial y}=0 \tag{17}$$

$$\frac{\partial u}{\partial y}=\left(\frac{\partial T}{\partial y}-Nr\frac{\partial C}{\partial y}-Rb\frac{\partial n}{\partial y}\right)\lambda\sin x \tag{18}$$

$$u\frac{\partial T}{\partial x}+v\frac{\partial T}{\partial y}=\frac{\partial^2 T}{\partial y^2}+Nb\frac{\partial T}{\partial y}\frac{\partial C}{\partial y}+Nt\left(\frac{\partial T}{\partial y}\right)^2 \tag{19}$$

$$Le\left(u\frac{\partial C}{\partial x}+v\frac{\partial C}{\partial y}\right)=\frac{\partial^2 C}{\partial y^2}+\frac{Nt}{Nb}\frac{\partial^2 T}{\partial y^2} \tag{20}$$

$$u\frac{\partial n}{\partial x}+v\frac{\partial n}{\partial y}+\frac{Pb}{Lb}\frac{\partial}{\partial y}\left((\sigma+n)\frac{\partial C}{\partial y}\right)=\frac{1}{Lb}\frac{\partial^2 n}{\partial y^2} \tag{21}$$

where Eq. (17) is used to obtain Eq. (21). The boundary conditions (15) become

$$\begin{aligned} &v(x,y)=0,\quad T(x,y)=1,\quad C(x,y)=1,\quad n(x,y)=1 \quad \text{at} \quad y=0,\quad 0\le x\le \pi \\ &u(x,y)\to u_e(x),\quad T(x,y)\to 0,\ C(x,y)\to 0,\ n(x,y)\to 0 \quad \text{as} \quad y\to\infty,\quad 0\le x\le \pi \end{aligned} \tag{22}$$

where we assume that $u_e(x)=\sin x$ (see Merkin (1977)). Here λ is the constant mixed convection parameter, Lb is the bioconvection Lewis number, Le is the traditional Lewis number, Pb is the bioconvection Péclet number, Nr is the buoyancy ratio parameter, Rb is the bioconvection Rayleigh number, Nb is the Brownian motion parameter, Nt is the thermophoresis parameter and σ is the motile parameter which are defined as

$$\begin{aligned} &\lambda=\frac{Ra}{Pe},\quad Lb=\frac{\alpha_m}{D_n},\quad Le=\frac{\alpha_m}{D_B},\quad Pb=\frac{bW_c}{D_n},\quad Nr=\frac{(\rho_p-\rho_{f\infty})\Delta\bar{C}}{\rho_{f\infty}(1-\bar{C}_\infty)\beta\Delta\bar{T}} \\ &Rb=\frac{\gamma\Delta\bar{n}\,\Delta\rho}{\rho_{f\infty}\beta\Delta\bar{T}},\quad Nb=\frac{\tau D_B\Delta\bar{C}}{\alpha_m},\quad Nt=\frac{\tau D_T\Delta\bar{T}}{\alpha_m\bar{T}_\infty},\quad \sigma=\frac{\bar{n}_\infty}{\Delta\bar{n}} \end{aligned} \tag{23}$$

with $Ra=(1-\bar{C}_\infty)\,g\,K\,\rho_{f\infty}\,\beta\Delta T\,a/(\mu\alpha_m)$ being the modified Rayleigh number for the porous medium. It is worth mentioning that $\lambda>0$ for an assisting flow ($T_w>T_\infty$), $\lambda<0$ for an opposing flow ($T_w<T_\infty$) and $\lambda=0$ for the forced convection flow, respectively. Integrating Eq. (18) and using the boundary conditions (22), we obtain

$$u=\sin x+(T-Nr\,C-Rb\,n)\lambda\sin x \tag{24}$$

In order to solve Eqs. (17), (19-21) and (24), we follow the method proposed by Merkin (1977) and introduce the following variables:

$$\psi=x\,f(x,y),\quad T=\theta(x,y),\quad C=\phi(x,y),\quad n=\chi(x,y) \tag{25}$$

where ψ is the stream function, which is defined in the usual way as $u=\partial\psi/\partial y$ and $v=-\partial\psi/\partial x$. Substituting the variables (25) into Eqs. (19-21) and (24), we obtain

$$\frac{\partial f}{\partial y}=\left[1+(\theta-Nr\,\phi-Rb\,\chi)\lambda\right]\frac{\sin x}{x} \tag{26}$$

$$\frac{\partial^2\theta}{\partial y^2}+f\frac{\partial\theta}{\partial y}+Nb\frac{\partial\theta}{\partial y}\frac{\partial\phi}{\partial y}+Nt\left(\frac{\partial\theta}{\partial y}\right)^2=x\left(\frac{\partial f}{\partial y}\frac{\partial\theta}{\partial x}-\frac{\partial f}{\partial x}\frac{\partial\theta}{\partial y}\right) \tag{27}$$

$$\frac{\partial^2\phi}{\partial y^2}+Le\,f\frac{\partial\phi}{\partial y}+\frac{Nt}{Nb}\frac{\partial^2\theta}{\partial y^2}=x\,Le\left(\frac{\partial f}{\partial y}\frac{\partial\phi}{\partial x}-\frac{\partial f}{\partial x}\frac{\partial\phi}{\partial y}\right) \tag{28}$$

$$\frac{1}{Lb}\frac{\partial^2\chi}{\partial y^2}+f\frac{\partial\chi}{\partial y}-\frac{Pb}{Lb}\frac{\partial}{\partial y}\left((\sigma+\chi)\frac{\partial\phi}{\partial y}\right)=x\left(\frac{\partial f}{\partial y}\frac{\partial\chi}{\partial x}-\frac{\partial f}{\partial x}\frac{\partial\chi}{\partial y}\right) \tag{29}$$

with the boundary conditions

$$\begin{aligned} &f(x,y)=0,\quad \theta(x,y)=1,\quad \phi(x,y)=1,\quad \chi(x,y)=1 \quad \text{at} \quad y=0,\quad 0\le x\le\pi \\ &f'(x,y)\to\frac{\sin x}{x},\quad \theta(x,y)\to 0,\quad \phi(x,y)\to 0,\ \chi(x,y)\to 0,\ \text{as}\ y\to\infty,\ 0\le x\le\pi \end{aligned} \tag{30}$$

It can be seen that near the lower stagnation point of the cylinder, i.e. $x\approx 0$, Eqs. (26-29) reduce to the following ordinary differential equations:

$$f'=1+(\theta-Nr\,\phi-Rb\,\chi)\lambda \tag{31}$$

$$\theta''+f\,\theta'+Nb\,\theta'\phi'+Nt\,\theta'^2=0 \tag{32}$$

$$\phi''+Le\,f\,\phi'+\frac{Nt}{Nb}\theta''=0 \tag{33}$$

$$\chi''+Lb\,f\,\chi'-Pb\left[\chi'\phi'+(\sigma+\chi)\phi''\right]=0 \tag{34}$$

with the boundary conditions (30) become

$$\begin{aligned} &f=0,\quad \theta=1,\quad \phi=1,\quad \chi=1 \quad \text{at} \quad y=0 \\ &f'=1,\quad \theta\to 0,\quad \phi\to 0,\quad \chi\to 0,\quad \text{as} \quad y\to\infty \end{aligned} \tag{35}$$

where primes denote differentiation with respect to y.

The quantities of practical interest in this study are the skin friction coefficient C_f, the local Nusselt number Nu_x, the local Sherwood number Sh_x and the local density number of the motile microorganisms Nn_x which are defined as

$$C_f=\frac{\overline{\tau}_w}{\rho\,\overline{u}_e^2},\quad Nu_x=\frac{\overline{x}}{k\,\Delta\overline{T}},\quad Sh_x=\frac{\overline{x}\,\overline{q}_m}{D_B\,\Delta\overline{C}},\quad Nn_x=\frac{\overline{x}\,\overline{q}_n}{D_n\,\Delta\overline{n}} \tag{36}$$

where $\overline{q}_w$, $\overline{q}_m$, and $\overline{q}_n$ are the wall heat, the wall mass and the wall motile microorganisms fluxes, respectively, and are defined as

$$\overline{\tau}_w=\mu\left(\frac{\partial\overline{u}}{\partial\overline{y}}\right)_{\overline{y}=0},\ \overline{q}_w=-k\left(\frac{\partial\overline{T}}{\partial\overline{y}}\right)_{\overline{y}=0},\ \overline{q}_m=-D_B\left(\frac{\partial\overline{C}}{\partial\overline{y}}\right)_{\overline{y}=0},\ \overline{q}_n=-D_n\left(\frac{\partial\overline{n}}{\partial\overline{y}}\right)_{\overline{y}=0} \tag{37}$$

Using variables (16) and (24), we obtain

$$(Pe_x^{1/2}/\mathrm{Pr})\,C_f = \frac{\partial f}{\partial y}(x,0), \quad Pe_x^{-1/2}\,Nu_x = -\frac{\partial \theta}{\partial y}(x,0)$$
$$Pe_x^{-1/2}\,Sh_x = -\frac{\partial \phi}{\partial y}(x,0), \quad Pe_x^{-1/2}\,Nn_x = -\frac{\partial \chi}{\partial y}(x,0) \tag{38}$$

where $Pe_x = \bar{u}_e(\bar{x})\bar{x}/\alpha_m$ is the local Péclet number. At the lower stagnation point of the cylinder, i.e. $x \approx 0$, the quantities of practical interest reduce to

$$(Pe_x^{1/2}/\mathrm{Pr})\,C_f = f'(0), \quad Pe_x^{-1/2}\,Nu_x = -\theta'(0)$$
$$Pe_x^{-1/2}\,Sh_x = -\phi'(0), \quad Pe_x^{-1/2}\,Nn_x = -\chi'(0)$$

where primes denote differentiation with respect to y.

3. Results and Discussion

At the lower stagnation point of the cylinder, i.e. $x \approx 0$, Eqs. (31-34) subject to the boundary conditions (35) have been solved numerically for different values of the parameters, namely the mixed convection parameter λ, the bioconvection Lewis number Lb, the traditional Lewis number Le, the bioconvection Péclet number Pb, the buoyancy ratio Nr, the bioconvection Rayleigh number Rb, the Brownian motion Nb and the thermophoresis Nt, using an efficient implicit finite-difference scheme known as the Keller-box method along with the Newton's linearisation technique as described by Cebeci and Bradshaw (1984) for both the assisting ($\lambda>0$) and opposing ($\lambda<0$) flow cases. The specific ranges of the dimensionless variables chosen for numerical computations were based on the existing literature values (Aziz *et al.* 2012). On the other hand, it is worth mentioning that we have considered the value of the motile parameter s = 1 throughout the computations.

In order to verify the accuracy of the present method, we have compared the present values of the heat transfer coefficient $-\theta'(0)$ with those reported by Cheng (1977) and Nazar *et al.* (2003) for regular Newtonian fluid at various values of λ, as presented in Table 1. We found that the comparison between these results are in excellent agreement. As such, we are confident that the present numerical method used and the results obtained are reliable.

Table 1: Values of $-\theta'(0)$ when $Rb = 0$, $Lb = 0$, $Le = 0$, $Nb = 0$, $Nr = 0$, $Nt = 0$, $Pb = 0$, $\sigma = 0$ (regular Newtonian fluid) and various values of λ

	$-\theta'(0)$		
λ	Cheng (1977)	Nazar *et al.* (2003)	Present
-1.1	0.4192	0.4193	0.4192
-1.0	0.4697	0.4698	0.4696
-0.5	0.6575	0.6576	0.6575
0	0.7980	0.7980	0.7979
0.5	0.9157	0.9156	0.9156
1.0	1.0192	1.0191	1.0191
2.0	1.1988	1.1987	1.1987
3.0	1.3543	1.3541	1.3542
4.0	1.4934	1.4932	1.4932
5.0	1.6204	1.6202	1.6202

To be continued...

...Continuation

10.0	2.1451	2.1444	2.1445
20.0	2.9243	2.9223	2.9232

It is observed from Table 2 that for sufficiently large negative values of λ or sufficiently cold cylinder, there will not be a boundary layer on the cylinder. It is shown that the largest considered bioconvection Rayleigh number ($Rb = 0.3$) has the furthest existing negative values of λ, which has a larger range to sustain as laminar flow during the opposing flow case, before the boundary layer starts to separate.

Table 2: Values of $Pe_x^{-1/2}Nu_x$, $Pe_x^{-1/2}Sh_x$ and $Pe_x^{-1/2}Nn_x$ when $Rb = 0.1$, 0.3 and 0.5, $Lb = 1$, $Le = 5$, $Nb = 0.1$, $Nr = 0.1$, $Nt = 0.1$, $Pb = 1$, $\sigma = 1$ and various values of λ

	$Pe_x^{-1/2}Nu_x$			$Pe_x^{-1/2}Sh_x$			$Pe_x^{-1/2}Nn_x$		
λ	$Rb = 0.1$	$Rb = 0.2$	$Rb = 0.3$	$Rb = 0.1$	$Rb = 0.2$	$Rb = 0.3$	$Rb = 0.1$	$Rb = 0.2$	$Rb = 0.3$
-2.4			0.2480			0.3415			0.5975
-2.2			0.2655			0.4135			0.7624
-2.0			0.2895			0.5050			0.9682
-1.8		0.2938	0.3234		0.4091	0.6187		0.t7198	1.2186
-1.6		0.3355	0.3675		0.5576	0.7486		1.0530	1.4989
-1.4	0.3137	0.3857	0.4168	0.4780	0.7204	0.8814	0.8787	1.4105	1.7808
-1.2	0.3910	0.4392	0.4660	0.7112	0.8794	1.0075	1.3866	1.7542	2.0464
-1.0	0.4588	0.4914	0.5128	0.9088	1.0263	1.1246	1.8117	2.0685	2.2916
-0.8	0.5187	0.5407	0.5569	1.0786	1.1605	1.2331	2.1748	2.3537	2.5182
-0.6	0.5724	0.5869	0.5983	1.2286	1.2835	1.3342	2.4943	2.6142	2.7289
-0.4	0.6215	0.6302	0.6373	1.3639	1.3973	1.4289	2.7817	2.8545	2.9261
-0.2	0.6669	0.6710	0.6742	1.4879	1.5034	1.5182	3.0446	3.0781	3.1121
0	0.7094	0.7096	0.7094	1.6030	1.6031	1.6030	3.2883	3.2878	3.2883
0.2	0.7494	0.7464	0.7429	1.7107	1.6974	1.6837	3.5162	3.4863	3.4561
0.4	0.7873	0.7814	0.7751	1.8123	1.7869	1.7609	3.7312	3.6740	3.6166
0.6	0.8235	0.8150	0.8060	1.9086	1.8724	1.8350	3.9351	3.8535	3.7707
0.8	0.8581	0.8473	0.8358	2.0006	1.9543	1.9063	4.1287	4.0253	3.9188
1.0	0.8913	0.8784	0.8646	2.0886	2.0330	1.9752	4.3143	4.1904	4.0618
1.2	0.9233	0.9084	0.8924	2.1731	2.1090	2.0418	4.4926	4.3496	4.2001
1.4	0.9543	0.9375	0.9195	2.2513	2.1822	2.1064	4.6624	4.5030	4.3343
1.6	0.9842	0.9657	0.9458	2.3332	2.2533	2.1691	4.8301	4.6517	4.4643
1.8	1.0133	0.9931	0.9713	2.4093	2.3222	2.2301	4.9905	4.7960	4.5909
2.0	1.0415	1.0198	0.9963	2.4832	2.3891	2.2895	5.1461	4.9362	4.7143
3.0	1.1724	1.1440	1.1126	2.8243	2.6998	2.5665	5.8639	5.5859	5.2889
4.0	1.2899	1.2559	1.2357	3.1291	2.9788	2.8190	6.5047	6.1692	5.7776
5.0	1.3976	1.3587	1.3273	3.4071	3.2345	3.0482	7.0890	6.7032	6.2604

Figure 1 shows the comparison of the effect of nanofluid and bioconvection parameters on different dimensionless profiles with regular base fluid case. We observed that the velocity profile has more significant impact, possibly due to the bioconvection phenomena, the average density of upwardly swimming microorganisms is slightly larger than that of water.

Figures 2 to 4 illustrate the effects of bioconvection parameters on the velocity profiles. It is observed that, for the assisting flow case, the velocity profile decreases at the surface with an increase in the bioconvection Rayleigh number; while it increases for the opposing flow case. For the assisting flow, due to the bioconvection plumes (a phenomenom of downward motion of the fluid), and plus the buoyancy factor, an oppose upward motion of the nanofluid occurs, and as a result, the velocity decreases as Rb increases.

Figure 2 shows that the velocity profile depends on the buoyancy ratio parameter, Nr and the bioconvection Rayleigh number Rb. During the assisting flow, the velocity profile

slightly increases relatively as the buoyancy ratio parameter *Nr* increases. The effects of the bioconvection parameters *Lb* and *Pb* along with *Rb* are shown in Figs. 3 and 4, respectively. The velocity profile eventually slightly decreases relatively as *Lb* increases, and increases relatively as *Pb* increases.

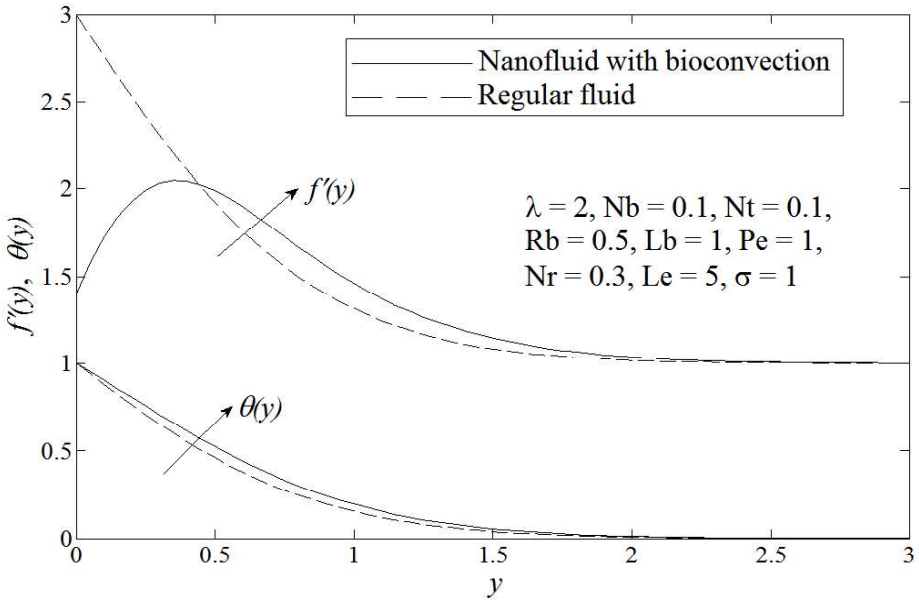

Figure 1: Effect of nanofluid and bioconvection parameters on the velocity, temperature, nanoparticle concentration profiles

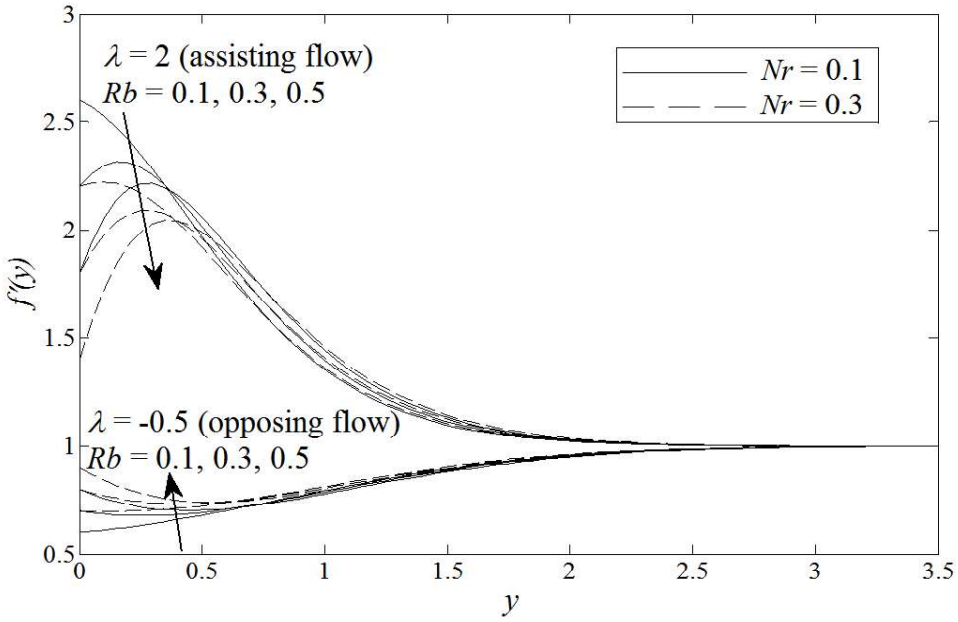

Figure 2: Effect of bioconvection Rayleigh number and buoyancy parameters on the velocity profiles, for the assisting and opposing flows

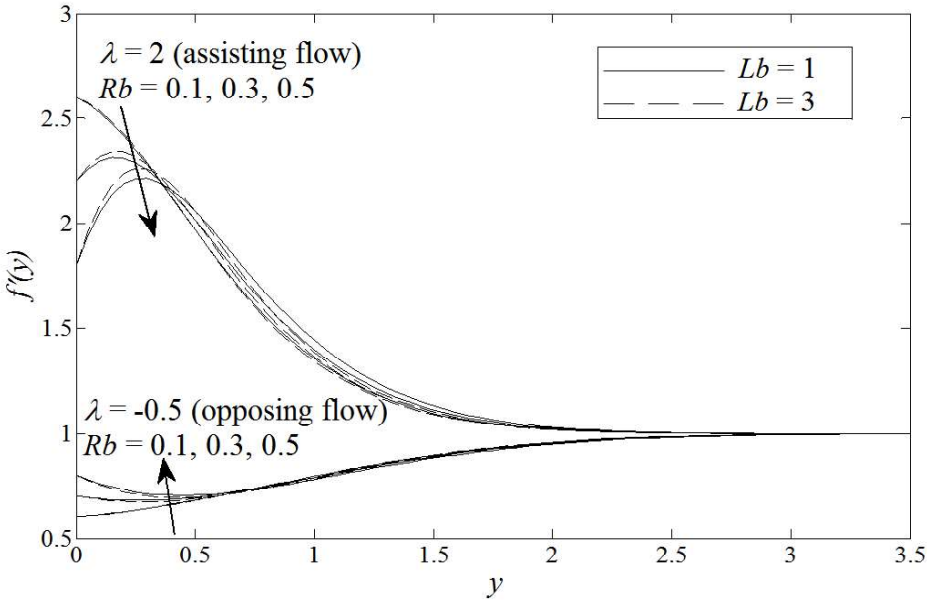

Figure 3: Effect of bioconvection Rayleigh and Lewis numbers on the velocity profiles, for the assisting and opposing flows

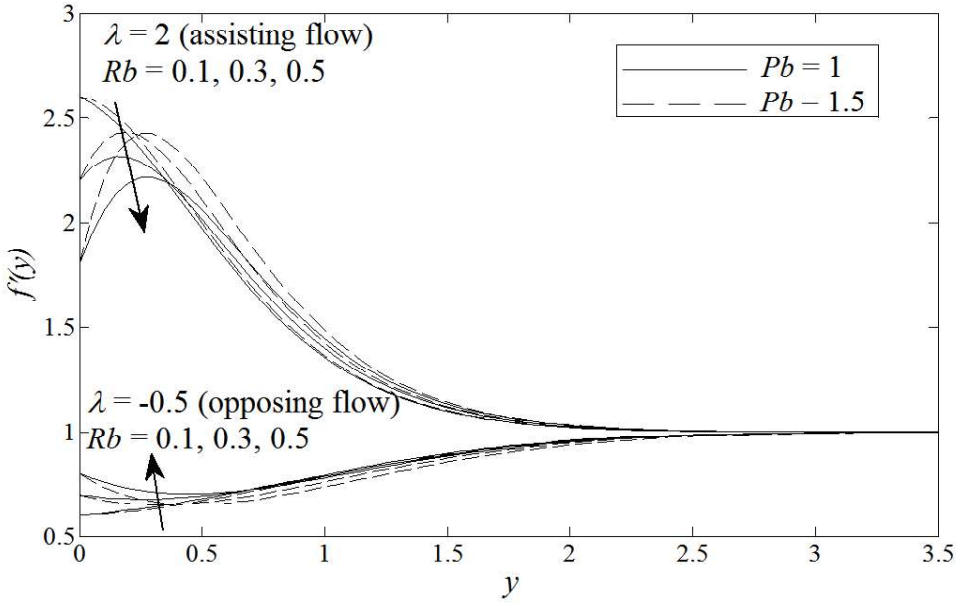

Figure 4: Effect of bioconvection Rayleigh and Péclet numbers on the velocity profiles, for the assisting and opposing flows

Figures 5 to 7 illustrate the effects of the bioconvection parameters on the temperature profiles. The temperature profiles appeared to be weakly dependent on all the *Rb*, *Nr*, *Lb* and *Pb* parameters. On the other hand, the opposite result occurs for the assisting flow, namely as *Rb*, *Nr*, *Lb* and *Pb* parameters increase, the temperature profile decreases.

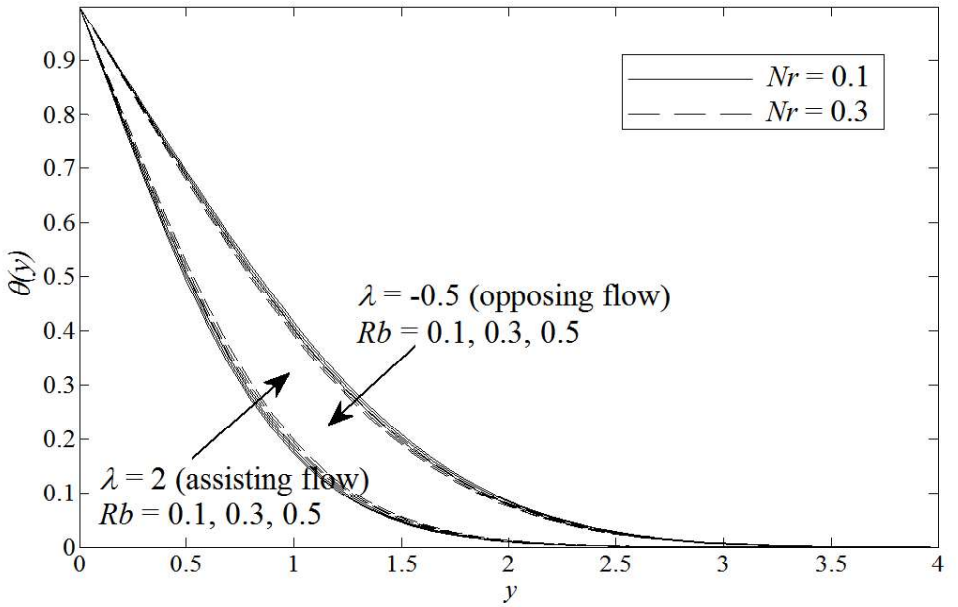

Figure 5: Effect of bioconvection Rayleigh number and buoyancy parameters on the temperature profiles, for the assisting and opposing flows

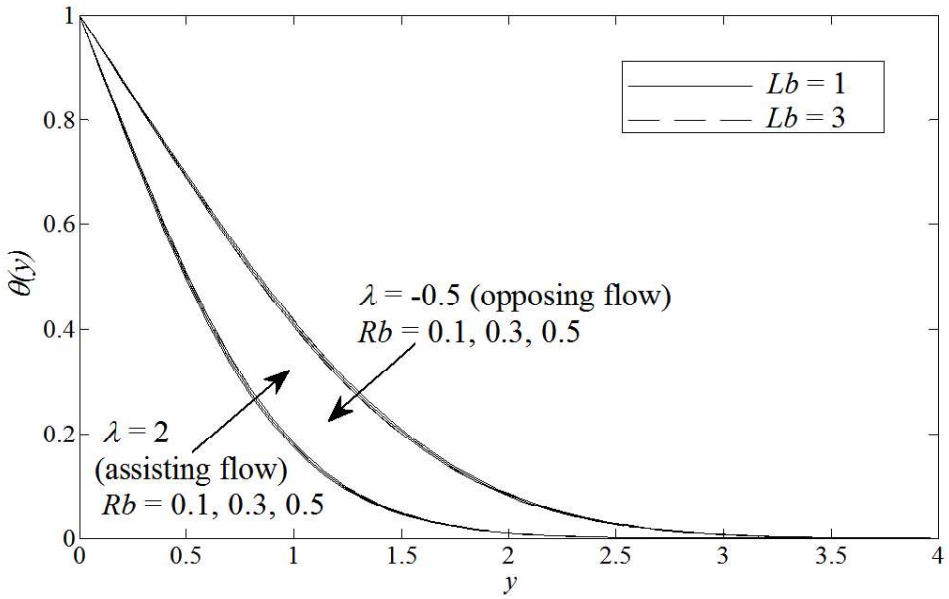

Figure 6: Effect of bioconvection Rayleigh and Lewis numbers on the temperature profiles, for the assisting and opposing flows

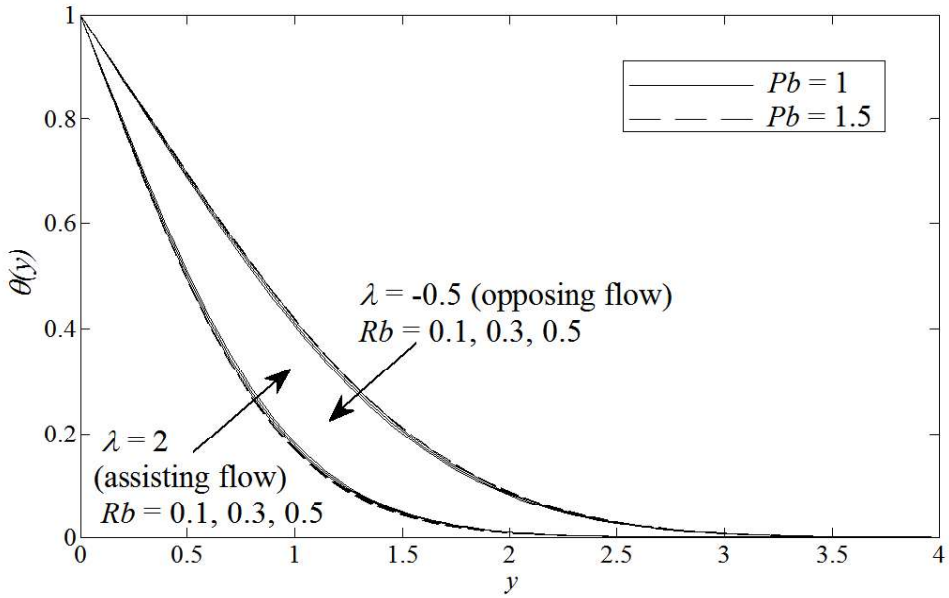

Figure 7: Effect of bioconvection Rayleigh and Péclet numbers on the temperature profiles, for the assisting and opposing flows

Figures 8 to 10 show the effects of bioconvection parameters on the nanoparticle concentration profiles. The nanoparticle concentration profiles are weakly dependent on all the *Rb*, *Nr*, *Lb* and *Pb* parameters. However, for the assisting flow, as *Rb*, *Nr*, *Lb* and *Pb* parameters increase, the temperature profile decreases; and the opposite pattern occurs for the opposing flow.

Figures 11 to 13 present the effects of bioconvection parameters on the density of motile microorganisms profiles. The density of motile microorganisms profiles are relatively sensitive and strongly influenced by the changes in *Lb*-*Rb* and *Pb*-*Rb*, which can be seen in Figs. 12 and 13, while for the assisting flow, as *Rb*, *Nr*, *Lb* and *Pb* parameters increase, the motile microorganisms profile decreases; and the opposite pattern occurs for the opposing flow.

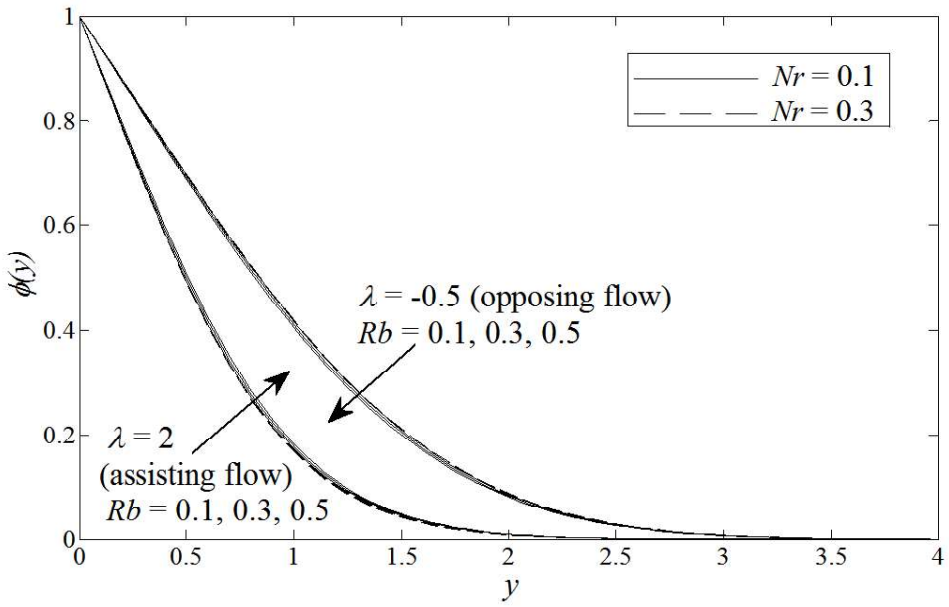

Figure 8: Effect of bioconvection Rayleigh number and buoyancy parameters on the nanoparticle concentration profiles, for the assisting and opposing flows

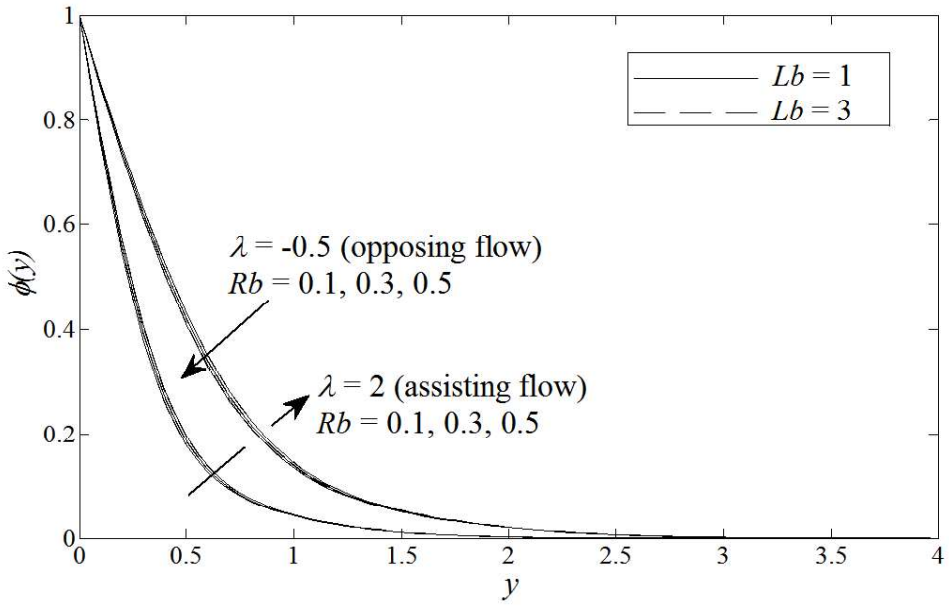

Figure 9: Effect of bioconvection Rayleigh and Lewis numbers on the nanoparticle concentration profiles, for the assisting and opposing flows

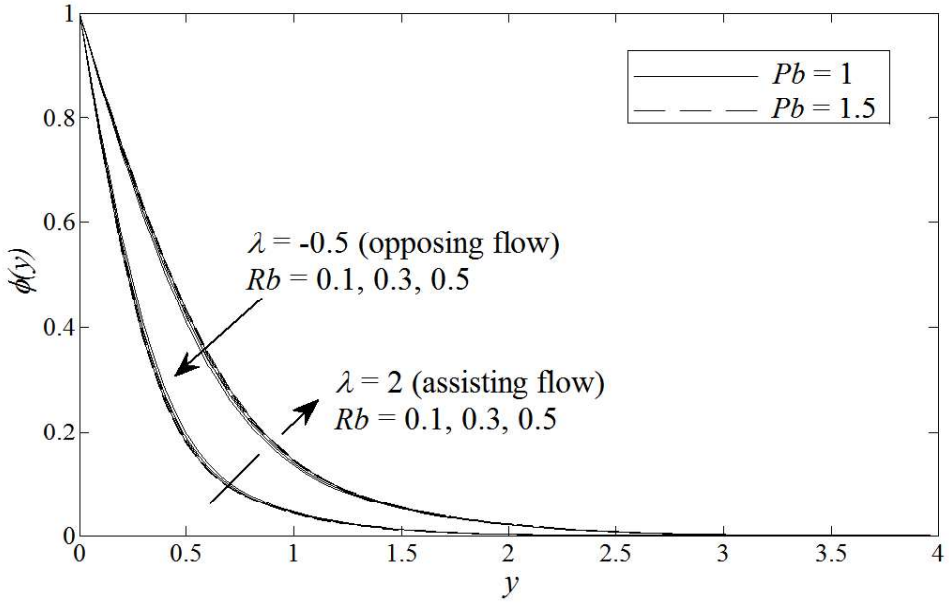

Figure 10: Effect of bioconvection Rayleigh and Péclet numbers on the nanoparticle concentration profiles, for the assisting and opposing flows

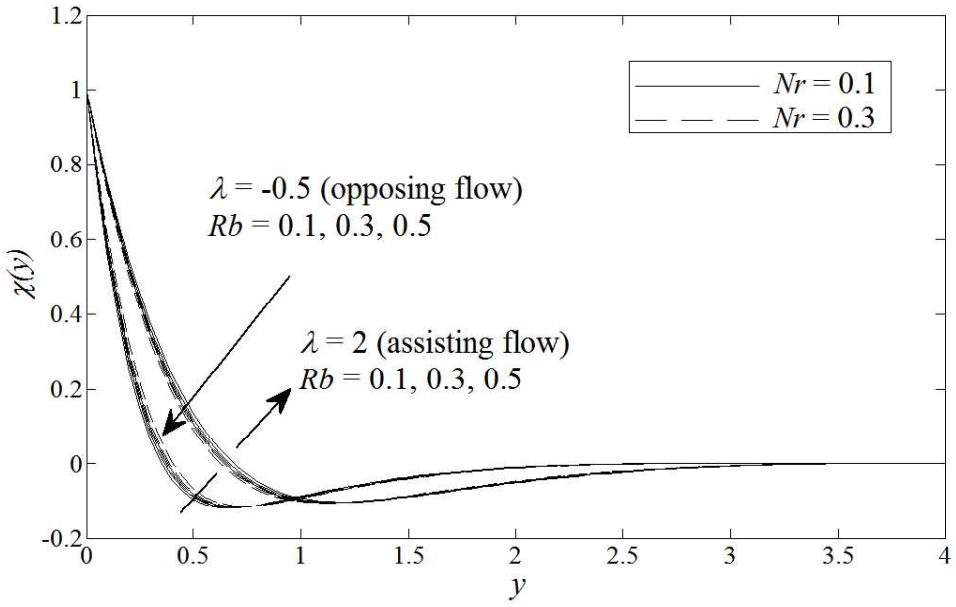

Figure 11: Effect of bioconvection Rayleigh number and buoyancy parameters on the microorganism profiles, for the assisting and opposing flows

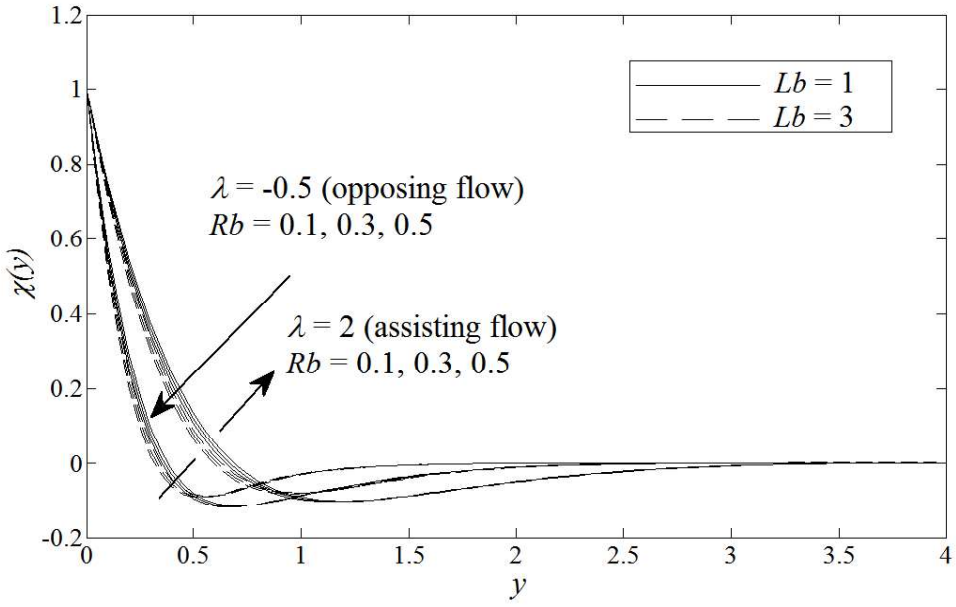

Figure 12: Effect of bioconvection Rayleigh and Lewis numbers on the microorganism profiles, for the assisting and opposing flows

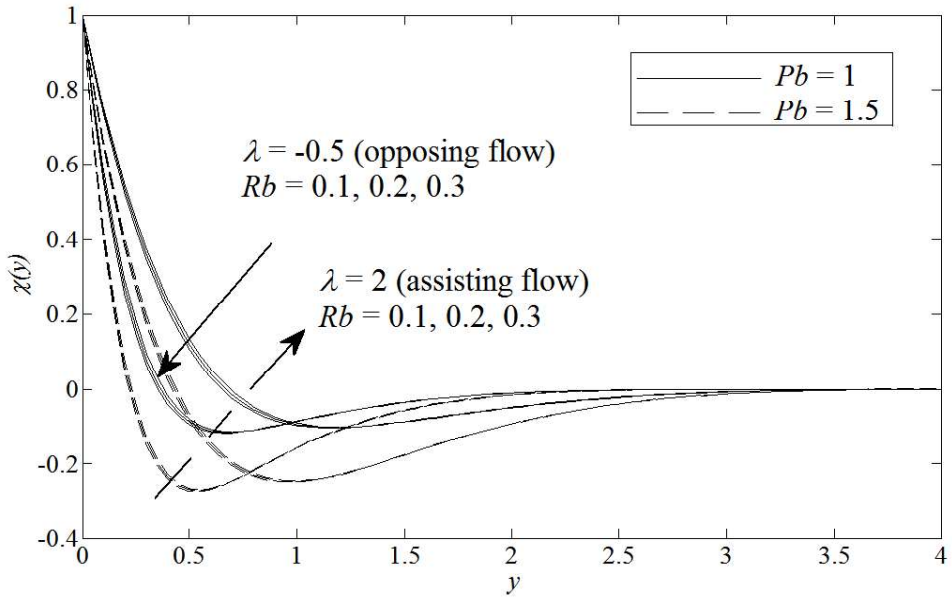

Figure 13: Effect of bioconvection Rayleigh and Péclet numbers on the microorganism profiles, for the assisting and opposing flows

4. Conclusions

In this paper, we have studied the problem of steady laminar mixed convection boundary layer flow over an isothermal horizontal circular embedded in a porous medium filled by a nanofluid containing gyrotactic microorganisms at lower stagnation point of the cylinder. We have looked into the effects of the mixed convection parameter λ, the bioconvection Lewis number *Lb*, the traditional Lewis number *Le*, the bioconvection Péclet number *Pb*, the buoyancy ratio *Nr*, the bioconvection Rayleigh number *Rb*, the Brownian motion *Nb* and the thermophoresis *Nt* on the velocity, temperature, nanoparticle concentration and microorganism distributions in the flow field. The governing boundary layer equations were solved numerically using the Keller-box method. From this study, we could draw the following conclusions:

• The numerical data indicates no significant effect of the bioconvection parameters on the temperature and nanoparticle concentration distributions in the flow field. However, the bioconvection Péclet number *Pb* have a significant impact on the velocity and density of motile microorganisms profiles.

• For the assisting flow, the local Nusselt number, Sherwood number and density number of the motile microorganisms decrease as *Rb* increases.

• For the opposing flow, the local Nusselt number, Sherwood number and density number of the motile microorganisms increases as *Rb* increases.

Acknowledgement

The authors would like to acknowledge the financial support received in the form of fundamental research grant scheme (FRGS/1/2011/SG/UKM/02/18) from the Ministry of Higher Education, Malaysia.

References

Aziz A., Khan W.A. & Pop I. 2012. Free convection boundary layer flow past a horizontal flat plate embedded in porous medium filled by nanofluid containing gyrotactic microorganisms. *Int. J. Therm. Sci.* **56**: 48-57.

Badr H.M. & Pop I. 1988. Combined convection from an isothermal horizontal rod buried in a porous medium. *Int. J. Heat Mass Transfer* **31**: 2527-2541.

Badr H.M. & Pop I. 1992. Effect of flow direction on mixed convection from a horizontal rod embedded in a porous medium. *Can. Soc. Mech. Eng. Transactions (CSME)* **16**: 267-290.

Bradean R., Ingham D.B., Heggs P.J. & Pop I. 1998. Mixed convection adjacent to a suddently heated horizontal circular cylinder embedded in a porous medium. *Trans. Porous Med.* **32**: 329-355.

Buongiorno J. 2006. Convective transport in nanofluids. *ASME J. Heat Transfer* **128**: 240-250.

Cebeci T. & Bradshaw P. 1984. *Physical and Computational Aspects of Convective Heat Transfer*. New York: Springer.

Cheng P. 1977. Combined free and forced convection flow about inclined surfaces in porous media. *Int. J. Heat Mass Transfer* **20**: 807-814.

Cheng P. 1982. Mixed convection about a horizontal cylinder and a sphere in a fluid saturated porous medium. *Int. J. Heat Mass Transfer* **25**: 1245-1247.

Choi S. 1995. Enhancing thermal conductivity of fluids with nanoparticles, in: *The Proceedings of the 1995 ASME International Mechanical Engineering Congress and Exposition*. San Francisco, USA, ASME, FED 231/MD, 99-105.

Das S.K., Choi S.U.S., Yu W. & Pradet T. 2007. *Nanofluids: Science and Technology*. New Jersey: Wiley.

Duangthongsuk W. & Wongwises S. 2007. A critical review of convective heat transfer nanofluids. *Renew. Sust. Eng. Rev.* **11**: 797-817.

Ghasemi B. & Aminossadati S.M. 2010. Periodic natural convection in a nanofluid-filled enclosure with oscillating heat flux. *Int. J. Therm. Sci.* **49**: 1-9.

Hillesdon A.J. & Pedley T.J. 1996. Bioconvection in suspensions of oxytactic bacteria: linear theory. *J. Fluid Mech.* **324**: 223-259.

Ingham D.B. & Pop I. (eds.). 2005. *Transport Phenomena in Porous Media, vol. III.* Oxford: Elsevier.

Kakaç S. & Pramuanjaroenkij A. 2009. Review of convective heat transfer enhancement with nanofluids. *Int. J. Heat Mass Transfer* **52**: 3187-3196.

Khanafer K., Vafai K. & Lightstone M. 2003. Buoyancy-driven heat transfer enhancement in a two-dimensional enclosure utilizing nanofluids. *Int. J. Heat Fluid Flow* **46**: 3639-3653.

Kumari M. & Pop I. 2009. Mixed convection boundary layer flow past a horizontal circular cylinder embedded in a bidisperse porous medium. *Trans. Porous Med.* **77**: 287-303.

Kuznetsov A.V. 2010. The onset nanofluid bioconvection in a suspension containing both nanoparticles and gyrotactic microorganisms. *Int. Commun. Heat Mass Transfer* **37**: 1421-1425.

Kuznetsov A.V. 2011. Non-oscillatory and oscillatory nanofluid bio-thermal convection in a horizontal layer of finite depth. *Eur. J. Mech. B-fluid* **30**: 156-165.

Merkin J.H. 1977. Mixed convection from a horizontal circular cylinder. *Int. J. Heat Mass Transfer* **20**: 73-77.

Nazar R., Amin N. & Pop I. 2003. The Brinkman model for the mixed convection boundary layer flow past a horizontal circular cylinder in a porous medium. *Int. J. Heat Mass Transfer* **46**: 3167-3178.

Nazar R., Tham L., Pop I. & Ingham D.B. 2011. Mixed convection boundary layer flow from a horizontal circular cylinder embedded in a porous medium filled with a nanofluid. *Trans. Porous Med.* **86**: 517-536.

Nield D.A. & Bejan A. 2006. *Convection in Porous Media.* 3rd Ed. New York: Springer.

Pedley T.J., Hill N.A. & Kessler J.O. 1988. The growth of bioconvection patterns in a uniform suspension of gyrotactic microorganisms. *J. Fluid Mech.* **195**: 223-237.

Sadik K. & Pramuanjaroenkij A. 2009. Review of convective heat transfer enhancement with nanofluids. *Int. J. Heat Mass Transfer* **52**: 3187-3196.

Sokolov A., Goldstein R.E., Feldchtein F.I. & Aranson I.S. 2009. Enhanced mixing and spatial instability in concentrated bacterial suspensions. *Phys. Rev. E* **80**: 031903.

Tsai T., Liou D., Kuo L. & Chen P. 2009. Rapid mixing between ferro-nanofluid and water in a semi-active Y-type micromixer. *Sensors Actuators A* **153**: 267-273.
Vafai K. (ed.). 2005. *Handbook of Porous Media*. 2nd Ed. New York: Taylor and Francis.
Wang X.Q. & Mujumdar A.S. 2007. Heat transfer characteristics of nanofluids: a review. *Int. J. Therm. Sci.* **46**: 1-19.
Wang X.Q. & Mujumdar A.S. 2008. A review on nanofluids – Part I: theoretical and numerical investigations. *Brazilian J. Chem. Eng.* **25**: 613-630.
Yu W. & Xie H.Q. 2012. A review on nanofluids: preparation, stability mechanisms, and applications. *J. Nanometer* **doi**:10.1155/2012/435873.

[1]Fakulti Industri Asas Tani
Universiti Malaysia Kelantan
Kampus Jeli
17600 Jeli
Kelantan DN, MALAYSIA
Mel-e: leonytham@gmail.com

[2]Pusat Pengajian Sains Matematik
Fakulti Sains dan Teknologi
Universiti Kebangsaan Malaysia
43600 UKM Bangi
Selangor DE, MALAYSIA
*Mel-e: rmn@ukm.my**

[3]Faculty of Mathematics
University of Cluj
R-3400 Cluj, CP-253
ROMANIA
E-mail: popm.ioan@yahoo.co.uk

** Corresponding author*